

# The impact of polar mesoscale storms on northeast Atlantic Ocean circulation

Alan Condron<sup>1</sup> and Ian A. Renfrew<sup>2\*</sup>

**Atmospheric processes regulate the formation of deep water in the subpolar North Atlantic Ocean and hence influence the large-scale ocean circulation<sup>1</sup>. Every year thousands of mesoscale storms, termed polar lows, cross this climatically sensitive region of the ocean. These storms are often either too small or too short-lived to be captured in meteorological reanalyses or numerical models<sup>2–4</sup>. Here we present simulations with a global, eddy-permitting ocean/sea-ice circulation model, run with and without a parameterization of polar lows. The parameterization reproduces the high wind speeds and heat fluxes observed in polar lows as well as their integrated effects, and leads to increases in the simulated depth, frequency and area of deep convection in the Nordic seas, which in turn leads to a larger northward transport of heat into the region, and southward transport of deep water through Denmark Strait. We conclude that polar lows are important for the large-scale ocean circulation and should be accounted for in short-term climate predictions. Recent studies<sup>3,4</sup> predict a decrease in the number of polar lows over the northeast Atlantic in the twenty-first century that would imply a reduction in deep convection and a potential weakening of the Atlantic meridional overturning circulation.**

Polar lows are mesoscale (<1,000 km diameter) low-pressure systems that occur throughout the world's subpolar seas, but tend to cluster in the North Atlantic over the Nordic (Greenland, Iceland, Norwegian) and Irminger seas<sup>4–7</sup>. Here minor differences in atmospheric forcing are sufficient to alter the density of the surface waters, such that the rate at which water sinks to depth is changed<sup>1</sup>. This ventilation process, known as deep open-ocean convection, is one of the fundamental mechanisms responsible for the renewal of North Atlantic Deep Water (NADW)—the major deep-water mass driving the Atlantic meridional overturning circulation<sup>8</sup> (AMOC).

Polar lows are not generally well resolved in global meteorological analyses, reanalyses or climate models owing to their small scales (typically ~250 km) and short lifetimes (typically 24–48 h; refs 2–4). Yet, the most intense polar lows are associated with localized gale force winds and heat losses from the ocean >1,000 W m<sup>-2</sup>, sufficient to significantly change the underlying ocean<sup>9–12</sup>. For brevity we will use the term polar low to encompass all polar mesoscale cyclones. We note, however, that in the literature<sup>13</sup> the term polar low is usually reserved for more intense polar mesoscale cyclones with wind speeds >15 m s<sup>-1</sup>. Many climate models predict that anthropogenic increases in atmospheric carbon dioxide will slow down the AMOC (ref. 14). However, in omitting polar lows, climate models are, at present, deficient at forcing the ocean over the critical deep-water formation regions of the subpolar seas, limiting confidence in their predictions.

We use a state-of-the-art, global, high-resolution (1/6°, ~18 km), eddy-permitting, ocean/sea-ice circulation model (MITgcm; ref. 15; see Methods) to determine the impact of polar lows on ocean circulation. At this resolution, the model represents the boundary currents and deep-water overflows of the subpolar seas that are crucial for NADW formation and the AMOC (refs 16,17); circulation features that were poorly resolved in a previous coarser-resolution two-year pilot study of the impact of polar lows on the ocean<sup>10</sup> (see Supplementary Discussion). Perturbation and Control ocean model experiments, with and without polar lows over the northeast Atlantic (50° N–80° N, 50° W–50° E) respectively, were run for 21 years (1978–1998) starting from identical ocean states. Thus, any differences between the simulations can be attributed to the impact of polar lows on the ocean. In the Perturbation integration ~60,000 polar lows are parameterized into the surface wind fields (see Supplementary Discussion and Fig. S1). The mean cyclone density (Fig. 1) compares well to existing polar-low climatologies determined using a variety of vortex identification techniques<sup>5–7</sup>.

Compelling evidence for the parameterization's overall veracity is provided by one-dimensional power spectra of the wind fields (Fig. 2). The Control spectrum has far too little power at scales below ~300 km owing to an inability of the atmospheric forcing fields to resolve storms below this scale. The Perturbation spectrum has considerably more power between 50 and 400 km, bringing it into line with what is observed<sup>18,19</sup>. Hence, the Perturbation experiment will receive the correct amount of wind forcing at scales of 50–400 km.

Inspection of the mixed-layer depth (a proxy for the depth of open-ocean convection) in the Nordic seas reveals that the localized increases in the surface heat flux provide sufficient cooling to destabilize the water column and trigger open-ocean convection on many more occasions and to greater depths (Fig. 3). Using a two-tailed *t*-test (see Methods and Supplementary Table S1 for a summary of all statistical test results) we find that the monthly mean changes in the depth to which open-ocean convection occurs in the Greenland, Norwegian and Iceland seas are all significantly different from the Control ( $p < 0.01$ ), with mean annual increases of monthly mixed-layer depths of 251, 121 and 160 m, respectively. Clearly, polar lows have a significant impact on ventilating the deep ocean. Figure 3a illustrates that the number of extra days each year with deep convection in the Greenland Sea correlates ( $r = 0.70$ ,  $p < 0.01$ ) with the number of polar lows occurring each winter (December–March). In the winter of 1993/1994, when there were an exceptionally large number of polar lows, the number of days with deep convection increased from 79 to 138. On average, the area of deep convection over the Greenland Sea increases by

<sup>1</sup>Climate System Research Center, Department of Geosciences, 233 Morrill Science Center, University of Massachusetts, Amherst, Massachusetts 01003-9297, USA, <sup>2</sup>School of Environmental Sciences, University of East Anglia, Norwich NR4 7TJ, UK. \*e-mail: I.Renfrew@uea.ac.uk

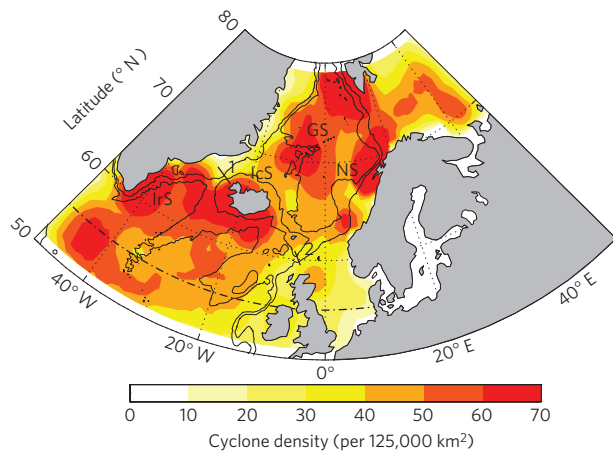


**Figure 1 | The annual mean density of polar lows over the northeast Atlantic Ocean.** Density from 1978 to 1998 (per 125,000 km<sup>2</sup>), in good agreement with a satellite-determined data set ( $r = 0.75$ ,  $p < 0.01$ ) and existing polar-low distributions using different identification techniques<sup>4–7</sup>, showing quantitatively similar features within the Irminger Sea, the lee of Greenland, south of Iceland, and in the central Norwegian and Greenland seas. Bathymetry is drawn at 500 and 2,000 m depths (black contour lines). The locations of the Greenland (GS), Norwegian (NS), Iceland (ICS) and Irminger (IRS) seas are marked. The sections used to calculate the volume of deep-water overflowing the GIS ridge are marked: (1) DSOW and (2) ISOW, and (dashed black line) the heat transport at 55° N. For heat transport, this section extends across the entire width of the Atlantic basin.

27% (~4,500 km<sup>2</sup>) and is deeper 97% of the time and by up to 2,000 m when polar lows are resolved (Fig. 3b). In the Norwegian Sea, convection is also deeper 97% of the time and by up to 1,000 m (Fig. 3c). In the Iceland Sea, there are similar changes (not shown) with the area undergoing deep convection increasing by an average of 41% (~1,050 km<sup>2</sup>) each year.

The inclusion of polar lows has a significant influence on the circulation of the Greenland Sea gyre. The gyre is composed of the northward flow of the warm, saline Norwegian–Spitzbergen Current, the southward flow of the cold, fresh East Greenland Current and the eastward flow of the Jan Mayen Current<sup>17</sup>. This cyclonic circulation facilitates open-ocean convection by allowing weakly stratified deep waters to be brought up (by thermal wind balance) and exposed to the surface forcing<sup>1</sup>. A barotropic streamfunction reveals that the gyre has (on average) a mean strength over the Greenland Sea of 3.5 Sv and an annual maximum (absolute) strength of 24.9 Sv. When polar lows are included, the monthly strength of the gyre averaged over the Greenland Sea increases 56% of the time during the 21-year integration; a two-tailed binomial test (see Methods) is significant at the 99% level, implying that stronger rotation is more frequent when polar lows are resolved. The impact of polar lows on the gyre is cumulative over time so that rotation is greater in 60% and 68% of months during the last 10 and 5 years, respectively; during the last 5 years of the Perturbation integration, the mean (absolute maximum) gyre strength is 8.2% (17.2%) stronger than the Control.

The changes in open-ocean deep convection are also reflected in the volume of Greenland Sea Deep Water (GSDW). After 21 years of forcing with polar lows there is a cumulative increase in GSDW of  $4.1 \times 10^3$  km<sup>3</sup> (5.3%), although a two-tailed binomial test indicates that it takes ~10 years for the volume of GSDW to become statistically greater than the Control integration ( $p < 0.01$ ). After 10 (15) years, the volume of GSDW is higher when polar lows are simulated in 61% (97%) of months; a two-tailed  $t$ -test indicates that the last 5 years are statistically different at the 95% confidence interval. The time lag emphasizes that both

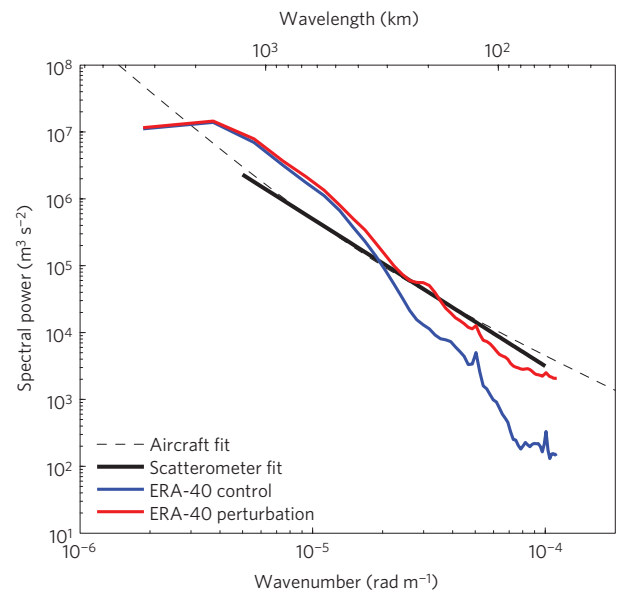


**Figure 2 | Power spectra of 10-m wind speed over the Nordic seas.** The lines show spectra for ERA-40 winds (blue line) and Perturbed ERA-40 winds (red line), where the perturbed winds have had polar lows added. The spectra are averages over approximately 20,000 lines, using data every 6 h for the month of January 1994 for a domain of 50° N–80° N, 20° W–20° E. Also plotted are a fit to aircraft observations of kinetic energy spectra<sup>18</sup> from the mid-latitudes and tropics (dashed black line), which is a  $k^{-5/3}$  power law in the mesoscale, and a fit to scatterometer-based 10-m wind observations for the mid-latitudes<sup>19</sup>, which is a  $k^{-2.2}$  power law (thick black line).

pre-conditioning of the ocean and the spin-up of the Greenland Sea gyre, due to surface forcing from polar lows, are key for deep-water mass formation<sup>1</sup>.

The increases in convection and deep-water production in the Nordic seas result in statistically significant increases in the transport of dense water overflowing the Greenland–Iceland–Scotland (GIS) ridge. The Control integration has a mean southward transport of Denmark Strait Overflow Water (DSOW) of 3.2 Sv that compares well to observations (3.07–3.68 Sv; ref. 20). When polar lows are simulated, DSOW transport is higher in 58% of months over the full 21 years and in 74% of months over the last 10 years, indicating that the effect of polar lows here is also cumulative over time. Figure 4a illustrates that monthly differences are up to  $\pm 0.5$  Sv ( $\pm 15\%$ ) and variability is high, but there is a clear trend towards the volume of deep-water overflowing the sill being ~0.1 Sv higher in the last ten years. A two-tailed binomial test for whether DSOW transport is statistically different for the 21-year period (that is, higher volume transport being more frequent with polar lows represented) is significant at the 99% level.

We find similar differences, and month-to-month variability, at the Faroe–Shetland Channel, with the volume of southward-flowing Iceland–Scotland Overflow Water (ISOW) greater when polar lows are simulated 59% (66%) of the time in the 21- (last 10-) year period. Again a two-tailed binomial test indicates that the increase in ISOW transport is statistically significant at the 99% level. The increased outflow at the GIS ridge is consistent with a lagged and nonlinear response to an increase in the hydraulic height of the reservoir of dense, deep water upstream in the Nordic seas<sup>8</sup>. The response in the volume transport of DSOW agrees with idealized modelling studies that show that an intensification of the wind forcing increases the volume transport at Denmark Strait, with both hydraulic control and wind stress forcing being important<sup>8,21</sup>.

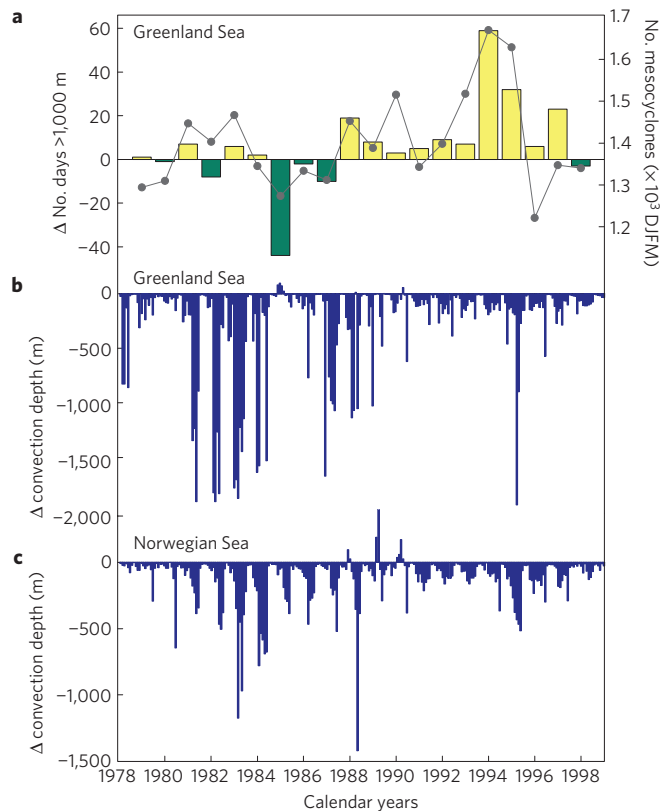


**Figure 3 | The impact of polar lows on open-ocean deep convection in the Nordic seas.** **a**, The difference (Perturbation minus Control) in the number of days each year (July–June) with open-ocean convection >1,000 m in the Greenland Sea (coloured bars), plus the number of polar lows each winter (December–March (DJFM); dark grey line) over the northeast Atlantic. **b,c**, The difference in the maximum depth of open-ocean convection each month in the Greenland Sea (**b**) and the Norwegian Sea (**c**).

South of the GIS ridge, the North Atlantic subpolar gyre (SPG) represents an important part of the AMOC and is composed of the warm, saline northward flow of the Gulf Stream and Irminger Current, the cold, fresh westward flow of the East and West Greenland Currents, and the cold, fresh, southward flow of the Labrador Current. The circulation of the gyre is maintained by buoyancy contrasts, wind forcing, and dense water overflows from the Nordic and Labrador seas<sup>22,23</sup>. Note that dense water from the Labrador Sea (Labrador Sea Water) is also formed by deep convection in the Irminger Sea<sup>17,24</sup>; and here including polar lows (Fig. 1) increases the mean annual monthly mixed-layer depth by 237 m. The strength of the SPG is calculated by averaging the monthly mean barotropic streamfunction over the entire gyre. The Control has a mean strength of 12.1 Sv. Including polar lows causes the gyre to spin-up by 0.47 Sv (3.9%) on average over the full 21 years and be stronger 80% of the time (Fig. 4b). After five years there is a more-or-less sustained increase in gyre strength, so that for the last 15 years the gyre is stronger 90% of the time by an average of 0.67 Sv (5.5%). The eastern part of the gyre (east of 50° W), that is, the part subject to direct polar low forcing, spins up by 0.56 Sv (4.6%) over the full 21 years and by 0.79 Sv (6.8%) over the last 15 years. The lagged increase in SPG strength, following an increase in mixed-layer depth in the Nordic seas, has been modelled previously<sup>23</sup> and attributed to the coupling of baroclinicity and the barotropic mode. A two-tailed *t*-test for the entire gyre and the eastern part show the 21-year averages to be significantly different ( $p < 0.02$  and  $p < 0.01$  respectively). In addition a two-tailed binomial test is significant at the 99% level,

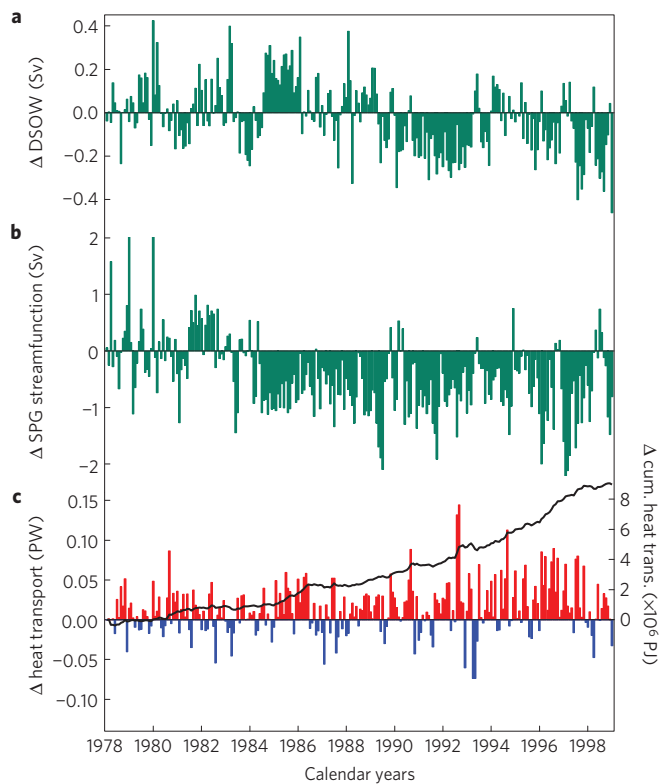


**Figure 4 | The impact of polar lows on monthly volume and heat transports in the North Atlantic.** **a**, The difference (Perturbation minus Control) in the volume of DSOw at Denmark Strait (negative values represent an increase in southward flow). There is a sustained increase in the volume of DSOw after 10 years when polar lows are resolved, leading to an extra  $3.2 \times 10^4 \text{ km}^3$  (3%) of deep-water reaching the North Atlantic. **b**, The difference in barotropic streamfunction of the subpolar gyre, highlighting that the entire gyre spins up when polar lows are included (negative values represent an increase in cyclonic rotation). **c**, The difference in northward heat transport at 55° N in the North Atlantic. Red (blue) colours indicate an increase (decrease) in heat transport. The cumulative difference in heat transport (black line) indicates that after 21 years an extra  $8.97 \times 10^6 \text{ PJ}$  of heat has been transported northwards owing to resolving polar lows.

confirming that resolving polar lows plays a key role in setting the pace of the SPG.

The spin-up of the SPG is accompanied by an increase in northward heat transport (Fig. 4c); at 55° N this is greater in 68% of months in the 21-year integration (statistically significant at the 95% confidence level in a two-tailed *t*-test and at the 99% level in a two-tailed binomial test). The impact of polar lows is again found to be cumulative so that for the last 15, 10 and 5 years the heat transport is greater in 70%, 74% and 75% of months, respectively. As a result, the average increase in heat transport over the last five years peaks at 0.025 PW (4%), which is statistically significant in a two-tailed *t*-test at the 95% level ( $p < 0.02$ ). During the 21-year integration, the persistent increase in northward heat transport leads to an extra  $8.97 \times 10^6 \text{ PJ}$  of heat being transported polewards.

Using a state-of-the-art ocean model capable of resolving narrow boundary currents, sills and overflows we find that mesoscale atmospheric forcing over the northeast Atlantic, in the form of parameterized polar lows, plays an important role in the circulation of the Nordic seas and subpolar North Atlantic. Our analysis of the surface and deep basins of the North Atlantic shows that polar lows are influencing the circulation of the Greenland Sea gyre and the frequency, depth and area of deep convection. This in turn increases

the formation of GSDW and the volume of DSOW flowing south at the GIS ridge. Finally, a spin-up of the SPG leads to a significant increase in the northward transport of heat to Europe and North America. On the basis of this scenario, our findings point towards polar lows as an important, yet absent, forcing in ocean, climate and seasonal forecasting models.

Under present Intergovernmental Panel on Climate Change future climate scenarios<sup>14</sup>, the number of polar lows is predicted to decrease over the Nordic seas and move northwards<sup>3,4</sup>. We surmise that such a shift would reduce the influence of polar lows on open-ocean deep convection in the Nordic seas, and so decrease the rate of GSDW formation and the volume of DSOW flowing into the North Atlantic. This could have a considerable effect on the deep waters of the North Atlantic, and potentially weaken the return branch of the AMOC.

## Methods

The MITgcm ocean model<sup>15</sup> is a coupled ocean/sea-ice free-surface, three-dimensional, primitive equation model that uses both the Boussinesq and the hydrostatic approximations. The ocean model is state-of-the-art, in particular being able to accurately represent near-shore boundary currents and the deep-water overflows of the subpolar seas that are crucial for simulating NADW formation and the return branch of the AMOC (refs 16,17). The model is placed on a cube-sphere grid projection that permits a relatively even grid spacing throughout the domain, and avoids polar singularities. The grid has a mean horizontal spacing of 18 km that is eddy-permitting, and there are 50 vertical levels, ranging in thickness from 10 m near the surface to approximately 450 m at the maximum model depth. Note that because the deformation radius in the North Atlantic is ~10–20 km, our model will not resolve all eddies, nor will it fully capture the restratification processes that occur following deep convection. The ocean model is coupled to the MITgcm sea-ice model, which follows a viscous-plastic rheology. The model was spun-up for 40 years from World Global Hydrographic Climatology data, optimized using a Green's function to minimize model/data residual. Control and Perturbation experiments were then run from this point, covering the forcing period 1 January 1978 to 31 December 1998, with no restoring to allow the ocean to freely evolve to the different atmospheric forcings. Note that the simulation length is a compromise between obtaining a sufficiently long ocean model run and concerns about model drift in what is a free-running ocean model.

In our analysis the Irminger Sea is defined as lying west of the Reykjanes Ridge to 43° W by 58° N–65.5° N; the Greenland Sea as 71.5° N–80° N by 17° W–30° E; the Norwegian Sea as 62° N–71.5° N by 5° W–17° E; and the Iceland Sea as 65.5° N–71.5° N by 40° W–5° W. Mixed-layer depths are used to determine the depth of open-ocean deep convection and are defined as the depth at which the density of a grid cell of ocean water is greater than the surface density by 0.125 kg m<sup>-3</sup>. Mixed-layer calculations are based on monthly differences averaged over each individual sea. GSDW is defined consistent with previous work<sup>17</sup> as water with a density  $\geq 1,028.07$  kg m<sup>-3</sup> within that part of the Greenland Sea where depth >2,000 m. The volume of GSDW is calculated from monthly mean salinity and potential temperature output. The formation rate of GSDW is based on month-to-month changes in the volume of GSDW. Note the formation rate of GSDW in the Control simulation is 0.12 Sv on average—in good agreement with the very broad range of rates (0.1–0.42 Sv) that is available from chlorofluorocarbon-based observations<sup>25,26</sup>. The transports at Denmark Strait and the Faroe-Shetland Channel are based on the volumes of water with densities  $\geq 1,027.8$  kg m<sup>-3</sup> flowing southwards through the cross-sections marked on Fig. 1, consistent with previous work<sup>8</sup>.

We make use of a two-sided *t*-test to test the null hypothesis that the data are independent random samples from normal distributions with equal means and equal, but unknown, variances, or the alternative hypothesis that the means are not equal. A significant result rejects the null hypothesis. We also make use of a two-tailed binomial test for the null hypothesis that the transports are not different in the Perturbation and Control integrations. A significant result rejects the null hypothesis. Note, where used, both of these statistical tests are applied to monthly mean data.

Received 23 June 2012; accepted 9 November 2012;  
published online 16 December 2012

## References

1. Marshall, J. & Schott, F. Open-ocean convection: Observations, theory, and models. *Rev. Geophys.* **37**, 1–64 (1999).
2. Condrón, A., Bigg, G. R. & Renfrew, I. A. Polar mesoscale cyclones in the Northeast Atlantic: Comparing climatologies from ERA-40 and satellite imagery. *Mon. Weath. Rev.* **134**, 1518–1533 (2006).

3. Kolstad, E. W. & Bracegirdle, T. J. Marine cold-air outbreaks in the future: An assessment of IPCC AR4 model results for the Northern Hemisphere. *Climate Dynam.* **30**, 871–885 (2008).
4. Zahn, M. & von Storch, H. Decreased frequency of North Atlantic polar lows associated with future climate warming. *Nature* **467**, 309–312 (2010).
5. Harold, J. M., Bigg, G. R. & Turner, J. Mesocyclone activity over the northeast Atlantic. Part 1: Vortex distribution and variability. *Int. J. Climatol.* **19**, 1187–1204 (1999).
6. Bracegirdle, T. J. & Gray, S. L. An objective climatology of the dynamical forcing of polar lows in the Nordic seas. *Int. J. Climatol.* **28**, 1903–1919 (2008).
7. Zahn, M. & Storch, H. von. A long-term climatology of North Atlantic Polar Lows. *Geophys. Res. Lett.* **35**, L22702 (2008).
8. Jungclauss, J. H., Macrander, A. & Kase, R. H. in *Arctic-Subarctic Ocean Fluxes: Defining the Role of the Northern Seas in Climate* (eds Dickson, R. R., Meincke, J. & Rhines, P.) 527–549 (Springer, 2008).
9. Shapiro, M. A., Fedor, L. S. & Hampel, T. Research aircraft measurements of a polar low over the Norwegian Sea. *Tellus* **37A**, 272–306 (1987).
10. Condrón, A., Bigg, G. R. & Renfrew, I. A. Modelling the impact of polar mesoscale cyclones on ocean circulation. *J. Geophys. Res.* **113**, C10005 (2008).
11. Saetra, O., Linders, T. & Deberbard, J. B. Can polar lows lead to a warming of the ocean surface? *Tellus A* **60**, 141–153 (2008).
12. Moore, G. W. K., Reader, M. C., York, J. & Sathiyamoorthy, S. Polar lows in the Labrador Sea: A case study. *Tellus* **48A**, 17–40 (1996).
13. Rasmussen, E. A. & Turner, J. *Polar Lows: Mesoscale Weather Systems in the Polar Regions* (Cambridge Univ. Press, 2003).
14. IPCC *Climate Change 2007: The Physical Science Basis* (eds Solomon, S. et al.) (Cambridge Univ. Press, 2007).
15. Marshall, J., Adcroft, A., Hill, C., Perelman, L. & Heisey, C. A finite-volume, incompressible Navier Stokes model for studies of the ocean on parallel computers. *J. Geophys. Res.* **102**, 5753–5766 (1997).
16. Schweckendiek, U. & Willebrand, J. Mechanisms affecting the overturning response in global warming simulations. *J. Clim.* **18**, 4925–4936 (2005).
17. Dickson, R. R., Meincke, J. & Rhines, P. *Arctic-Subarctic Ocean Fluxes: Defining the role of the northern seas in climate* (Springer, 2008).
18. Nastrom, G. D. & Gage, K. S. A climatology of atmospheric wavenumber spectra of wind and temperature observed by commercial aircraft. *J. Atmos. Sci.* **42**, 950–960 (1985).
19. Patoux, J. & Brown, R. A. Spectral analysis of QuikSCAT surface winds and two-dimensional turbulence. *J. Geophys. Res.* **106**, 23995–24005 (2001).
20. Macrander, A., Send, U., Valdimarsson, H., Jonsson, S. & Kase, R. H. Interannual changes in the overflow from the Nordic Seas into the Atlantic Ocean through Denmark Strait. *Geophys. Res. Lett.* **32**, L06606 (2005).
21. Biastoch, A., Kase, R. H. & Stammer, D. B. The sensitivity of the Greenland–Scotland ridge overflow to forcing changes. *J. Phys. Oceanogr.* **33**, 2307–2319 (2003).
22. Langehaus, H. R., Medhaug, I., Eldevik, T. & Helge-Ottera, O. Arctic/Atlantic exchanges via the subpolar gyre. *J. Clim.* **25**, 2421–2439 (2012).
23. Treguier, A. M. et al. The North Atlantic subpolar gyre in four high-resolution models. *J. Phys. Oceanogr.* **35**, 757–774 (2005).
24. Pickart, R. S., Spall, M. A., Ribergaard, M. H., Moore, G. W. K. & Milliff, R. F. Deep convection in the Irminger Sea forced by the Greenland tip jet. *Nature* **424**, 152–156 (2003).
25. Rhein, M. Convection in the Greenland Sea, 1982–1993. *J. Geophys. Res.* **101**, 18183–18192 (1996).
26. Schlosser, P., Bonisch, G., Rhein, M. & Bayer, R. Reduction of deepwater formation in the Greenland Sea during the 1980s: Evidence from Tracer Data. *Science* **251**, 1054–1056 (1991).

## Acknowledgements

The authors would like to thank G. R. Bigg, B. Harden, D. P. Stevens, G. W. K. Moore and P. E. Isachsen for useful discussion and comments. We acknowledge the ECMWF for providing the ERA-40 fields. The numerical model integrations used resources of the National Energy Research Scientific Computing Center, which is supported by the US DOE Office of Science under Contract No. DE-AC02-05CH11231.

## Author contributions

A.C. and I.A.R. jointly conceived the study. A.C. adapted the parameterization scheme and carried out the model runs and model output analysis. I.A.R. carried out the spectral analysis of the wind fields. A.C. and I.A.R. jointly interpreted the results and wrote the manuscript.

## Additional information

Supplementary information is available in the online version of the paper. Reprints and permissions information is available online at [www.nature.com/reprints](http://www.nature.com/reprints). Correspondence and requests for materials should be addressed to I.A.R.

## Competing financial interests

The authors declare no competing financial interests.